

Blob Transport at High Collisionality and the SOL Density Limit

D. A. D'Ippolito, J. R. Myra and D. A. Russell

Lodestar Research Corporation, 2400 Central Avenue, Boulder, Colorado 80301

June, 2006

*Presented at the 33rd EPS Conference on Plasma Physics,
Rome, Italy, June 19 - 23, 2006, Paper P5.160*

Blob Transport at High Collisionality and the SOL Density Limit

D. A. D'Ippolito, J.R. Myra, D. A. Russell

Lodestar Research Corporation, Boulder, Colorado, USA

1. INTRODUCTION

This paper describes recent developments in the theory of blob transport at high collisionality, $\Lambda = (v_{ei}L_{||}/\rho_s\Omega_e) \sim 1$, and its application to the convective density limit on Alcator C-Mod. The original sheath-connected blob model¹ described how coherent structures created by edge turbulence would charge up (due to ∇B and curvature drifts) and $E \times B$ drift across the far SOL. This model accounted for several qualitative observations about SOL turbulence, such as its spatial and temporal intermittency and non-diffusive SOL transport of particles and energy.

Several other blob parameter regimes have been identified,² which are relevant in the highly turbulent blob creation zone in the near SOL. In each regime, the radial blob velocity v_x has a known scaling with plasma parameters and with the blob radius a_b . This picture is unified by a simple *correspondence rule* between the linear dispersion relation of the underlying instability driving the turbulence and the blob parameters:

$$\gamma \rightarrow \frac{v_x}{a_b}, k_{\perp} \rightarrow \frac{1}{a_b}, L_n \rightarrow a_b , \quad (1)$$

where γ and k_{\perp} are the linear instability growth rate and wavenumber, and L_n is the density gradient scale length. This rule is obtained by assuming that the same physics drives the instability and the motion of the blob and by using a wave-breaking condition ($\omega \sim k \cdot v$) for saturation of the turbulence. One simple way to understand and visualize the diverse regimes is by considering the effective electrical circuit² of the current path satisfying $\nabla \cdot J = 0$ with the curvature drift providing a fixed source current; the effective resistivity of the circuit to loss currents determines γ (in linear theory) and v_x (in the nonlinear regime). This idea and the scaling in Eq. (1) makes explicit the correspondence between linear stability and turbulent transport noted in Ref. 3 for sheath-driven interchange modes and generalizes it to more collisional instability regimes.

2. THEORY AND SIMULATIONS

3D simulations^{4,5} and theoretical models^{2,6} have investigated several of the blob regimes and have shown that increasing the collisionality parameter Λ leads to electrical and thermal disconnection of the blobs from the sheaths. Disconnection increases the effective resistivity of the “blob circuit” ($\propto \Lambda$) and leads to faster radial propagation. In the

transition from the sheath-connected¹ (SC) regime to the resistive ballooning (RB) regime, the blob velocity is given by the resistive X-point (RX) regime scaling^{2,4}

$$v_x = q \Lambda / a_b^2 \quad (2)$$

in Bohm units ($v \rightarrow v/c_s$, $L \rightarrow L/p_s$) with $q = L_{\parallel}/R$. For $\Lambda > \Lambda_{\text{crit}} \equiv \min[1, \epsilon_x \Omega]$, the RX mode physics is important (see below) and $v_x \propto \Lambda$ showing that the blobs move faster as the collisionality increases. Here, $\Omega = (a_b/a_*)^{5/2}$, $a_* = L_{\parallel}^{2/5} / R^{1/5}$ (in Bohm units) and $\epsilon_x \ll 1$ is a “fanning factor” associated with the flux tube geometry near the X-point. In the RX regime, the current cannot flow along \mathbf{B} because of the larger parallel resistivity; the current loop closes via the ion polarization current, $\mathbf{J}_{\perp\text{pol}}$ near the X-points. The flow of \mathbf{J}_{\perp} is facilitated by the distortion of the flux tube into a thin fan near the X-point^{6,7} (note the factor ϵ_x in Λ_{crit}). For very large collisionality ($\Lambda \rightarrow \infty$), $\mathbf{J}_{\perp\text{pol}}$ closes the turbulent current loop in the midplane region (strong ballooning regime).⁸ Here, for fixed geometry we are interested in exploring the dependence of the transport on parameter space: (Λ, Ω) for initialized blobs and Λ for turbulence, which generates a range of scale sizes.

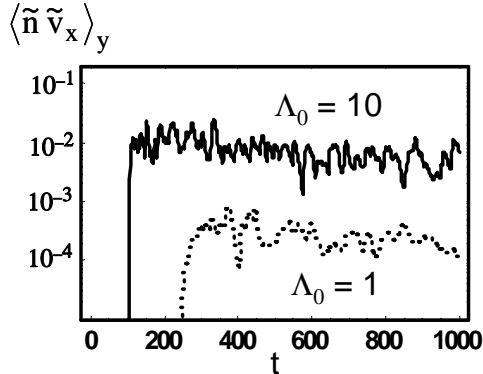


Fig. 1 Time history of the turbulent (blob) particle transport for two values of the collisionality parameter Λ_0 ($\Lambda_0 = \Lambda$ measured at the top of the density pedestal). Note the earlier onset of the nonlinear turbulent phase and the much larger particle flux for large Λ_0 .

For this purpose, we use a new 2-point 2D model that gives a reduced description of 3D turbulence.⁹ Implemented in a new version of the Lodestar SOLT code, a 2D simulation evolving (n, Φ) is carried out at two points along the field line (midplane and divertor) with boundary terms connecting the two regions. A dimensionless scaling analysis of the equations shows there are two invariant parameters (collisionality Λ and scale length, represented by Ω). The propagation of initialized cylindrical blobs [with density $n \sim \exp(-r^2/a_b^2)$] was simulated as a function of Λ and Ω retaining both regions, and it was shown that the numerical v_x agreed well with the analytic “blob dispersion relation” obtained from Eq. (1). Fully-turbulent simulations have studied the evolution of randomly seeded noise using a particle source term to maintain the profile gradient at the last closed flux surface. It is found that the qualitative character of the turbulence is sensitive to collisionality. Consistent with experiments^{10,11} and 3D simulations,^{4,5} the two-region code

shows a dramatic increase in the midplane fluctuating fields and turbulent particle flux $\langle \tilde{n} \tilde{v}_x \rangle_y$ with collisionality (see Fig. 1) due to disconnection (the ratio of fluctuating fields in the divertor region to that in the midplane region decreases for larger Λ). A wavelet analysis of the blob size distribution shows that the most probable blob size, $\langle a_b \rangle$, increases with Λ , and the dependence of $\langle v_x \rangle$ on $\langle a_b \rangle$ shows the qualitative dependence on Λ expected from the collisional blob theory.

3. DENSITY LIMIT MODEL

A similar two-point model for (T, Φ) was used in an analytic study of SOL heat balance and thermal density limits,¹² motivated by experiments on Alcator C-Mod.^{10,11} Assuming a cross-field heat flux $q_\perp \propto T_1^\mu / T_2^{v/2}$, the model exhibits a bifurcated equilibrium with warm and cold X-point roots when $v > 2\mu$. (The subscript denotes the region: 1 = midplane, 2 = divertor.) The normalized equilibrium heat fluxes for the two roots are plotted vs the parameter C_\perp in Fig. 2, taken from Ref. 12. Here, $C_\perp \propto n_1^2$ measures the cross-field blob transport ($\propto \Lambda$ in the RX-mode regime). The blob heat transport term ($\propto C_\perp T_1 / T_2^{3/2}$) adds the cold X-point root to the model. The warm X-point root is thermally stable, but the cold X-point root is thermally unstable (suffers thermal collapse), so their merger point defines an equilibrium limit on the SOL density (and collisionality). The thermal instability of the X-point in this model is analogous to an X-point Marfe, except that here the cooling is caused by turbulent (blob) heat transport rather than radiation. Note in Fig. 2 that Q_\perp/Q_{\parallel} increases with C_\perp and the stable (observable) hot X-point root reaches the equilibrium limit just after Q_\perp exceeds Q_{\parallel} , as observed on C-Mod. In fact, there is remarkable qualitative agreement between Fig. 2 and the data (compare with Fig. 18 of Ref. 11). There are several other points of agreement between the convective density limit model and the C-Mod experiments, as discussed in Ref. 12.

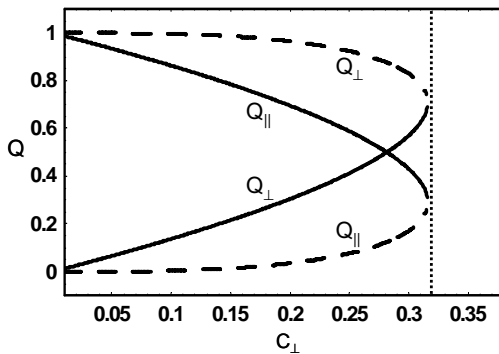


Fig. 2 Normalized heat flows Q_\perp , Q_{\parallel} vs C_\perp in thermal equilibrium for the “warm X-point” root (solid curves), and the “cold X-point” root (dashed). For the stable and physically-observable warm X-point root, Q_\perp exceeds Q_{\parallel} just before the equilibrium limit is reached, as observed in C-Mod.

4. SUMMARY AND DISCUSSION

We have described a new 2-point (midplane, divertor) 2D SOL model which is useful for both analytic and numerical studies of blobs with structure along \mathbf{B} . An important physics result of these studies is collisional disconnection by ion polarization currents, which results in a strong dependence of the turbulent transport on collisionality (see Fig. 1). Computations with this extended 2D model are much faster than running full 3D codes. In future work, the model will be extended to include parallel magnetic shear and the physics determining the blob size distribution and other statistics will be studied in detail.

New collisional blob regimes have been discussed which are valid in the blob creation zone (in the near SOL and edge) and allow description of strong resistive-ballooning turbulence. At high collisionality the turbulence has a shorter correlation length ($L_{\parallel} \sim \lambda_{ei}$) along the \mathbf{B} field and is not affected by whether the blob flux tube terminates in a sheath, passes an X-point or is part of a closed magnetic surface. In this limit, the physics of edge and SOL merge, the convective SOL transport moves across the last closed flux surface into the plasma edge, and the core confinement rapidly deteriorates. Thus, the collisional blob theory discussed in this paper agrees with the observed increase of edge turbulent transport with collisionality (see Fig. 1) and provides a mechanism for the convective density limit observed on C-Mod (see Fig. 2).

Finally, we note that in the collisional limit the blob theory agrees with standard turbulent transport estimates. It can be shown that the radial particle flux estimated from blob theory, $\Gamma \sim n v_x$, agrees in order of magnitude with mixing length theory, $\Gamma \sim Re[\tilde{n} \tilde{v}_x^*] \sim n \gamma / (k_{\perp}^2 L_n)$, when the blob correspondence rule (1) is used [e.g. see the discussion after Eq. (24) in Ref. 12].

This work was supported by the U.S. DOE grant DE-FG02-97ER54392.

- ¹ S. I. Krasheninnikov, Phys. Lett. A **283**, 368 (2001); D. A. D'Ippolito, J. R. Myra, and S. I. Krasheninnikov, Phys. Plasmas **9**, 222 (2002).
- ² J. R. Myra and D. A. D'Ippolito, Phys. Plasmas **12**, 092511 (2005).
- ³ M. Endler, H. Niedermeyer, *et al.*, Nucl. Fusion **35** 1307 (1995).
- ⁴ D. A. Russell, D. A. D'Ippolito, J. R. Myra, W. M. Nevins, X. Q. Xu, Phys. Rev. Lett. **93**, 265001 (2004).
- ⁵ X. Q. Xu, W. M. Nevins, T. D. Rognlien, *et al.*, Phys. Plasmas **10**, 1773 (2003).
- ⁶ S. I. Krasheninnikov, D. D. Ryutov, and G. Q. Yu, J. Plasma Fusion Res. **6**, 139 (2005).
- ⁷ D. Farina, R. Pozzoli, and D. D. Ryutov, Nucl. Fusion **33**, 1315 (1993).
- ⁸ O. E. Garcia, V. Naulin, A. H. Nielsen, and J. Juul Rasmussen, Phys. Rev. Lett. **92**, 165003 (2004).
- ⁹ D. A. Russell, D. A. D'Ippolito, and J. R. Myra, Bull. APS **50**, 84 (2005), paper CP1 45; J. R. Myra *et al.*, manuscript in preparation (2006).
- ¹⁰ B. LaBombard, R. L. Boivin, M. Greenwald, *et al.*, Phys. Plasmas **8**, 2107 (2001); M. Greenwald, Plasma Phys. Control. Fusion **44**, R27 (2002).
- ¹¹ B. LaBombard, J. W. Hughes, D. Mossessian, *et al.*, Nucl. Fusion **45**, 1658 (2005).
- ¹² D. A. D'Ippolito and J. R. Myra, LRC Report LRC-06-107, to be published in Phys. Plasmas **13**, (2006).